Article

Not peer-reviewed version

The Effect of Localized Magnetic Fields on the Spatially Controlled Crystallization of Organometallics and Transition Metal Complexes

Ian R. Butler * , Rhodri M. Williams , Alice Heeroma , Peter N. Horton , Simon J. Coles , Leigh F. Jones *

Posted Date: 3 March 2025

doi: 10.20944/preprints202502.2279.v1

Keywords: magnetic field; crystallization; inorganic; complex; nickel; patterns; zinc

doi:10.20944/preprints202502.2279.v1

Article

The Effect of Localized Magnetic Fields on the Spatially Controlled Crystallization of Organometallics and Transition Metal Complexes

Ian R. Butler [1,*] Rhodri M. Williams [1], Alice Heeroma [1], Peter N. Horton [2], Simon J. Coles [2] and Leigh F. Jones [1,3,*]

[1] School of Natural Sciences, Bangor University, Deiniol Road, Bangor. LL57 2DG, UK., Bangor University, Bangor, Gwynedd, U.K. LL57 2UW e-mail: i.r.butler@hotmail.co.uk; heeromaalice@gmail.com

[2] National Crystallography Service, School of Chemistry and Chemical Engineering, University of Southampton, Southampton, SO17 1BJ, UK; E-mail- p.n.horton@soton.ac.uk s.j.coles@soton.ac.uk

[3] School of Pharmacy and Life Sciences, Faculty of Science and Engineering, University of Wolverhampton, Wulfruna Street, Wolverhampton, WV1 1LY, UK. Email: Leigh.Jones@wlv.ac.uk. Tel: +44 01902-32-1180.

* Correspondence: i.r.butler@hotmail.co.uk (I..R.B.); leigh.jones@wlv.ac.uk (L.F.J.)

Abstract: The crystallization of nickel (II) bis-phosphine and nickel and zinc cluster complexes have been carried out in localized magnetic fields set up using neodymium magnets, including custom made Magnetic Crystallization Towers (MCTs). In all cases, whether the product complex is diamagnetic or paramagnetic, a complex spatial patterning of the crystals occurs based on the orientation of the magnetic field lines. The effects of nucleation, and solution concentration gradients on the crystallization process are also explored. These observations therefore show how the crystallization process is affected by magnetic fields and thus these results have far-reaching effects which most certainly will include crystallization and ion migrations in biology.

Keywords: magnetic field; crystallization; inorganic; complex; nickel; patterns; zinc

1. Introduction

One area of chemistry which has to some extent been neglected is chemistry in magnetic fields.[1–8] There are many biological phenomena associated with weak magnetic fields such as bird navigation and effects on the human body, yet the mechanism of these actions is still poorly understood. In chemistry the use of *epr/esr* spectroscopy play an important role in the study of materials in spectroscopic terms, however the bulk effects in solution in synthetic chemistry are less well studied. The work of Tesla and Faraday inspired generations of electromagnetic researchers, which has essentially taken us to where we are today in terms of electronic components. Despite the significant number of articles on single molecule magnets, [9–11] the linking of magnetochemistry to bulk synthesis is sorely lacking. One rather obvious application is the crystallization in magnetic fields. Several years ago (2015-17) we carried out the first of these experiments, which we can now report. We have undertaken a raft of experiments with both paramagnetic and diamagnetic compounds and have observed astonishing results. It is intuitively obvious that the crystallization of paramagnetic complexes in magnetic fields may provide interesting research results, but it is perhaps less obvious that diamagnetic compounds which are weakly repelled from magnetic fields should also show this effect that is until we realize that in all compounds electron motion will cause many localized fields which are susceptible to magnetic fields. The original inspiration for this work came from teaching demonstrations of the Meisner effect [12–14] where a static conventional ceramic superconductor clearly shows the effect of concerted magnetic repulsion but in a localized manner unlike that of conventional magnets where stabilization of the third degree of freedom is required. The other aspect which should also be obvious is that the different effects on the HOMO and LUMO molecular orbitals in a magnetic field should influence the course of a chemical reaction or at least be responsible for the catalysis of chemical reactions if a well- designed reactor can be built- clearly the very local effects of magnetic fields mean that the substrate -magnet distances should be short or chemistry in high magnetic fields could be carried out inside electromagnets. The other phenomenon which is clearly at play are the effects of local currents in the solutions because material transport in solution leading to concentration gradients are clearly important. In the present context, it is best to begin with pictorial representations of crystallisations in a magnetic field.

Magnetic fields, generated either by electromagnets or permanent commercially available magnets, have long been used to treat hardwater. [15–17] The application of a magnetic field has been shown to strongly influence fluid-flow hydrodynamics that in-turn directly affect aggregation and / or disaggregation of colloidal solids (e.g. calcite and aragonite from hardwater). [18] It is also believed that magnetic field effects significantly influence crystallisation processes in solution (of both diamagnetic and paramagnetic substances). For instance, the crystallisation of protein structures using external magnetic fields has become commonplace in protein crystallography and can be carried out in both solutions and gel media. [19–22] Indeed, a very recent and significant development demonstrated that hen egg white lysozyme (HEWL) could be crystallised in a contactless fashion through levitation (HEWL is suspended in a solution) using external magnets in the form of a "magnetic force booster." [23] Similarly, Whitesides and co-workers have employed Magneto-Archimeded levitation (MagLev) to separate mixtures of crystal polymorphs using density differentiation. This was achieved using a sophisticated self-built device comprising two permanent magnets (like-poles facing each other) separated by a void space that accommodates a sample cuvette containing the crystal mixture. [24] In 2019, the same device was successfully employed in the density driven separation and identification of illicit drugs at much lower quantities / concentrations (<50 mg) than are required using standard forensic methodologies. This was achieved using the MagLev phenomenon in combination with FT-IR and / or ^{1}H NMR.[25]

In a similar vein, Chen and co-workers have shown that the application of a strong magnetic field (90 kOe) during the preparation of the multiferroic formate perovskite $[(CH_3)_2NH_2][Mn(HCOO)_3]$ leads to slight topological changes within the resultant extended architecture and significant changes in magnetic behaviour. [26] Similarly, Hong and co-workers were able to introduce molecular disorder and important topological changes that encouraged altered magnetic behaviour within a $[Fe(1,4\text{-}dcb)(N(CN)_2)_2]$ complex (1,4-*dbc* = 1,4-dichlorobenzene). Interestingly, at higher magnetic fields (1 T) a complete breakdown of the complex was observed as indicated by the crystallisation of $Fe(ClO_4)_2{\cdot}6H_2O$ precursor. [27] In 2014, Meihaus and co-workers discovered that the nearby positioning of a permanent $Nd_2Fe_{13}B$ magnet promoted the crystallisation of the otherwise stubborn N_2^{3-} radical bridged lanthanide complexes $[\{(R_2N)_2(THF)Ln\}_2(\mu_3\text{-}\eta^2{:}\eta^2{:}\eta^2\text{-}N_2)K]$ (Ln = Gd, Tb, Dy; $NR_2 = N(SiMe_3)_2$) as opposed to the otherwise favoured non radical azide bridged analogue complexes. [28] Similarly, using a $Fe_{14}Nd_2B$ magnet, Higgins *et al* carried out extremely effective thermal gradient driven separation of both dia- and paramagentic rare-earth $[RE(TriNO_x)]$ complexes from complex mixtures. [29] In 2019, Naaman and co-workers employed a 0.52T permanent magnet to execute the enantiospecific crystallisation of amino acids (asparagine, glutamic acid hydrochloride and threonine). [30] In the same year, a potentially groundbreaking use for a permanent magnet was discovered when Galán-Mascarós and co- workers showed that the introduction of a moderate (≤450 mT) magnetic field at the anode (using a commercially available Nd magnet) significantly enhanced electrocatalytic water oxidation when using highly magnetic electrocatalysts. [31]

In the first paper we have chosen to illustrate the work using the nickel phosphine complexes [32–36] and heptanuclear pseudo metallocalix[6]arene complexes $[(MeOH)_2{\subset}Ni(II)_7(OH)_6(L)_6](NO_3)_2$ (CCDC = 758960) [37] and $[(MeOH)_2{\subset}Zn(II)_7(OH)_6(L)_6](NO_3)_2$ (where LH = 2-iminomethyl-6-methoxyphenol [38] which are readily available in our laboratories.

2. Results and Discussion

2.1. Part A Nickel Phosphine Complexes

The first complex we studied was the formation of the dark green paramagnetic complex [(*dppf*)$NiCl_2$], **1**, *dppf* = 1,1'-bis-(diphenylphosphino)ferrocene, [39] since this ligand was readily available in bulk in our laboratories. In all magnetic fields studied this complex crystallized anisotropically both in terms of crystal morphology and orientation. The typical magnetic field strengths used were 20-100 mtesla. In the first experiments a crystallizing solution in a small glass vial was placed either inside a circular stack of three neodymium magnets (40/23 mm, height 6 mm, neodymium, N42, nickel-plated, 21 kg), Figure 1, or touching a small stack of rectangular This section may be divided by subheadings.

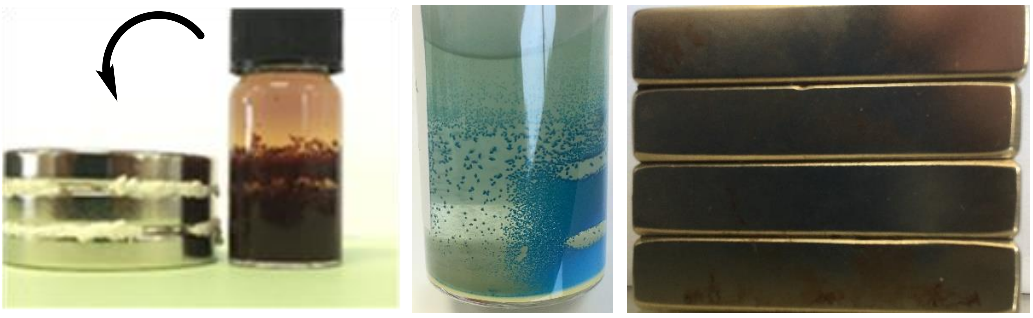

(**a**) (**b**)

Figure 1. (a) Crystallisation pattern of [Ni(*dppf*)Cl_2], 1, inside a stack of three ring magnets (b) A vial containing a crystallising solution of $[(C_6H_4\text{-}CH_2\underline{P}{}^tBu_2\text{-}2\text{-}C_6H_4\text{-}CH_2P(H){}^tBu_2)_2NiCl_3$ placed adjacent to a stack of 4 magnets. Smaller crystals are observed next to the magnet and distinct areas of little or no crystallisation is apparent.

It should provide a concise and precise description of the experimental results, their interpretation, as well as the experimental conclusions that can be drawn. magnets (block NdFeB, 30 x 15 x 6 mm, approx. 86.3 N, as shown in Figure 2 (RHS). The methodology chosen was one we have used for a considerable period which is the room temperature reaction of the yellow/orange anhydrous [Ni(DME)Cl_2] with the ligand. Even though the precursor complex is poorly soluble in most organic solvents we have successfully used it in dichloromethane at room temperature to form many complexes. In this case a dichloromethane slurry was used, and diethyl ether was added as a separate layer to facilitate the crystallization. The poor solubility means that the reaction is slow, however we did not want to introduce water. Each of these results indicate a clear crystallization pattern was observed for this nickel complex. (The magnetic field strengths of the magnets were measured on the exterior of the stacked magnets using a gaussmeter). The region where the crystals were observed were those which showed the highest field strengths and the areas where no crystals formed were those of low or zero magnet field. It should be mentioned at this point that we are looking at the formation of the tetrahedral paramagnetic nickel (II) dichloride complex which has been structurally characterized.[40] This complex has been used as a catalyst for many years. (N.B A nickel (I) complex has previously been crystallographically characterized also.) Encouraged by these results we turned our attention to the crystallization of the Zwitterionic complex $[(C_6H_4\text{-}CH_2\underline{\mathbf{P}}{}^tBu_2\text{-}2\text{-}C_6H_4\text{-}CH_2P(H){}^tBu_2)_2NiCl_3]$, **2**, which we were working on independently on a catalysis project.[41] Again, initially the crystallizing solution of this complex was placed adjacent to the stacked magnets and in this case the crystallization patterns were even more defined, as shown in Figure 2. Smaller crystals were formed near the magnet and larger crystals formed further away indicating that more nucleation was taking place adjacent to the magnets. In addition, there were noticeably clear areas adjacent to the magnets where there was no nucleation. Similarly, when $[(C_6H_4\text{-}CH_2\underline{\mathbf{P}}{}^tBu_2\text{-}2\text{-}C_6H_4\text{-}CH_2P(H){}^tBu_2)_2NiCl_3]$ was crystallized with magnetic spheres were placed around a vial of a crystallizing solution a distinct patterning was observed on the vial walls as shown in Figure 2a.

A similar crystallisation pattern was obtained when *dppf* was reacted with $[Ni(DME)Cl_2]$ to give $[($*dppf*$)NiCl_2]$. A close-up view is shown in Figure 2b.

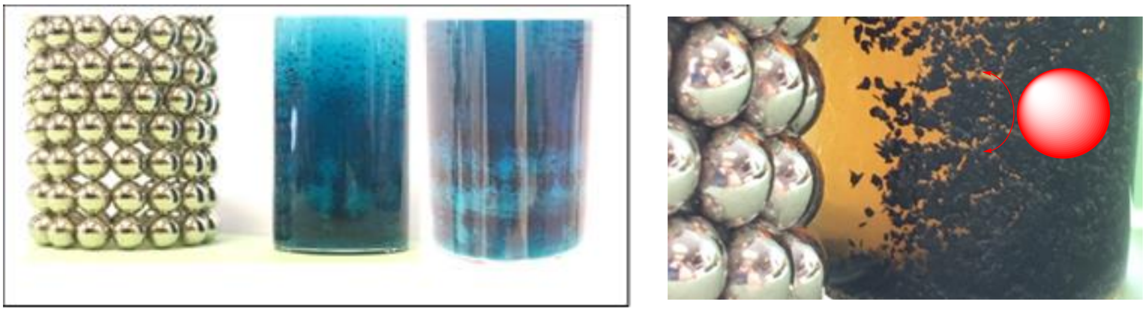

(**a**) (**b**)

Figure 2. (a) $[(C_6H_4\text{-}CH_2\underline{P}{}^tBu_2\text{-}2\text{-}C_6H_4\text{-}CH_2P(H){}^tBu_2)_2NiCl_3]$ crystallised in a vial surrounded by magnetic spheres. (b) A close-up view of the pattern obtained in the crystallisation of $[($*dppf*$)NiCl_2]$ in a vial surrounded by magnetic spheres, (the red inset shows the size of the spheres which were behind crystals).

The pattern may be independently visualised using magnetic field paper, as shown in Figure 3.

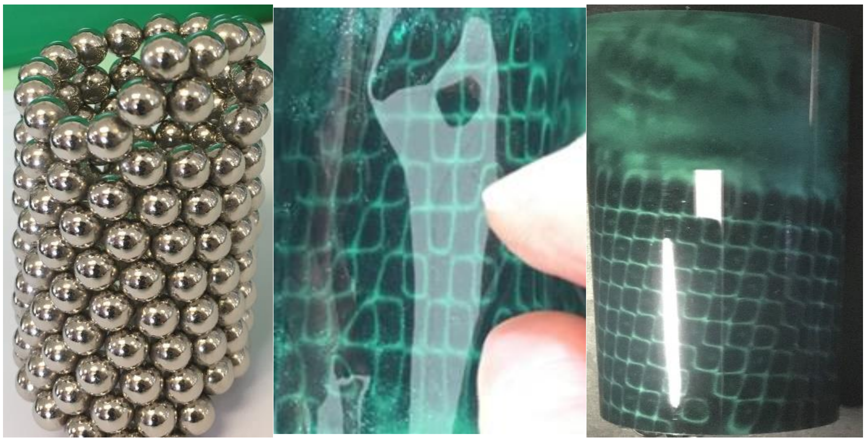

Figure 3. Visualisation of magnetic field pattern created by spheres using magnetic field paper.

Since $[(C_6H_4\text{-}CH_2\underline{\mathbf{P}}{}^tBu_2\text{-}2\text{-}C_6H_4\text{-}CH_2P(H){}^tBu_2)_2NiCl_3]$, again exhibited the crystallisation properties particularly well it was chosen to look at crystallisation in a round bottomed flask, placed on top of circular magnets as shown in Figure 4.

doi:10.20944/preprints202502.2279.v1

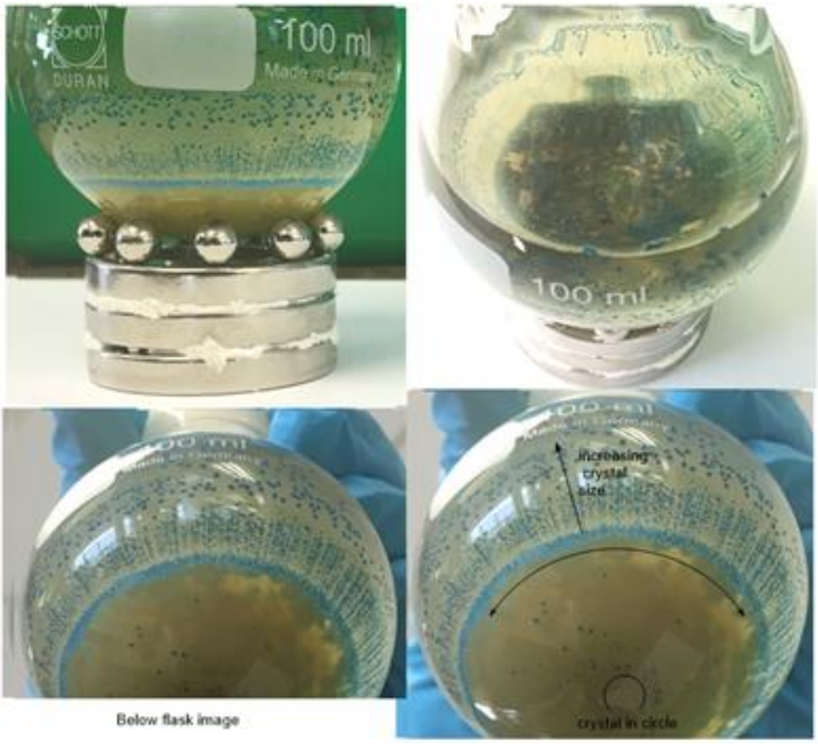

Figure 4. Crystallisation of $[(C_6H_4\text{-}CH_2\underline{P}{}^tBu_2\text{-}2\text{-}C_6H_4\text{-}CH_2P(H){}^tBu_2)_2NiCl_3]$ in a round bottomed flask on top of an array of circular and spherical magnets. Notice the concentric rings of crystals and the increase in the crystal size from top to bottom. (N.B the magnetic fields strengths may be seen in the supporting information).

This turned out to be the most visually appealing result with concentric rings of crystals produced. The larger crystals are those which form first at a distance from the magnet and the very small crystls adjacent to the magnet indicate an increase in nucleation near the magnet. Boyed by these results several complexes were examined including diamagnetic complexes and similar properties were observed in each case. The simplest of these are [Ni(*dppe*)Cl_2], [42,43] **3**, *dppe* = bis 1,2-diphenylphosphinoethane and [Ni(*dppp*)Cl_2],[44,45] *dppp* = 1,3-bis-diphenylphosphinopropane, complexes which are red/brown. It was found that these too crystallised in a well-defined 3D pattern. Although the product complexes are diamagnetic (square planar Ni(II) metal centres) it is important to remember that the patterning behaviour may be a result of diffusion of any intermediate complexes which may be paramagnetic. When the magnets were placed directly into the crystallizing solution crystal rings were observed, Figure 5a.

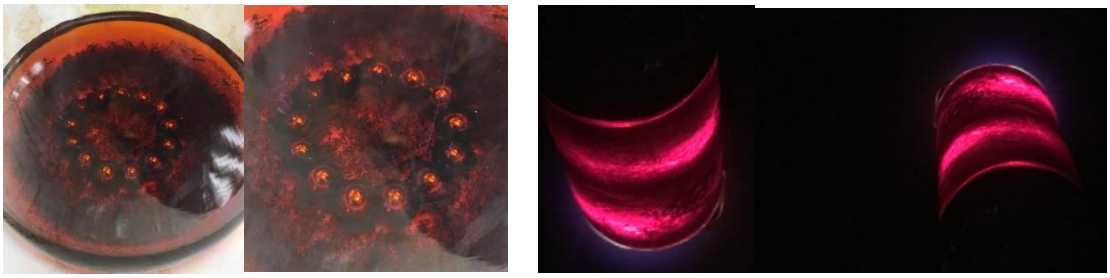
(**a**) (**b**)

Figure 5. a, Crystallisation of [Ni(*dppp*)Cl_2] around a circle of magnets **b**, Crystallisation of [Ni(*dppp*)Cl_2] in a vial within circular magnets- using light to show the crystallisation pattern.

In some cases where a very dense deeply coloured solution crystallises in a vial the human eye cannot detect an effect, but we observe that shining light through the sample reveals the crystallisation patterns, Figure 5b. At this point it is important to state that the crystallisation

Preprints.org (www.preprints.org) | NOT PEER-REVIEWED | Posted: 3 March 2025 doi:10.20944/preprints202502.2279.v1

phenomenon may be associated with the nickel precursor and thus the formation of a diamagnetic product does not necessarily mean that the phenomena apply to diamagnetic complexes. When the ligand *triphos* (*triphos* = tris- (methyldiphenylphosphino)methane) [46–49] was used we observed that the crystal formed grid pattern in the vial following field lines, Figure 6.

Figure 6. Crystallisation of [Ni *P,P*-(η^2- *triphos*)Cl_2] showing the crystals reaching into solution following field line patterns. These crystals form suspended fragile grids which collapse on agitation.

The crystals of 'NiTriphos' were shown to have a disordered nickel ion centre, with a mixture of either tetrahedral or square planar geometry (at 12:88 ratio), along with an associated disordered DCM solvate to compliment filling the cavity. (The split forms are shown in Figure 7). The unit cell is effectively a match with the known square planar complex [50,51] which although recrystallized from THF, shows no solvent in the structure but does contain suitable void spaces. Thus, it does appear as though the magnetic field is inducing some change of the nickel centres into the tetrahedral geometry.

(Two further crystals (TriphosNiCl$_2$_C2 and TriphosNiCl$_2$_ C3) have been attempted from that same batch which gave the same unit cell, and upon solving produce slightly different ratios (16:84 and 13:87)), showing that there is a little variation in the effect of the magnetic field as to the formation that occurs).

In one final case we looked at the formation and crystallisation of [$(PPh_3)_2NiCl_2$].[52] It is well known that it may form both tetrahedral and square planar complexes depending on the nature of the solvent used. We would expect in the square planar complex would form because we are using dichloromethane as solvent and indeed that is the case, but this apparently simple preparation turned out to be the most complex.

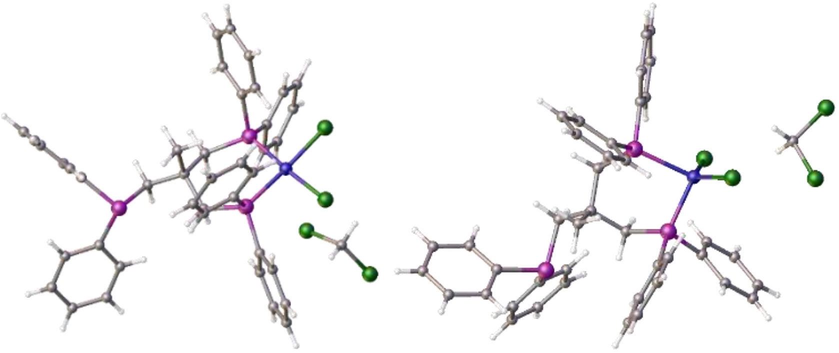

Figure 7. Tetrahedral and square planar complexes of *P,P*-[(1,1,1-tris(diphenylphosphinomethyl)ethane)NiCl$_2$]. (CCDC = 2422622). Full crystallographic data is given in the supplementary section).

We studied the formation over 20 times using even more powerful magnets and on many different scales; the crystallising solution indicated the presence of many powdered products in addition to the crystalline material. The solution was always violet coloured, yet an off-white precipitate also formed which we initially thought was ligand. However, this powder was stacked on the tube wall nearest the magnets and it could be physically moved inside the vial by moving the external magnets and it was strongly attracted to the external magnets in real time. This manifestation of bulk magnetic properties was an intriguing observation. The nature of this white powder is unknown and thus clearly this is an avenue of research which requires further exploration. Additional photographs of the crystallisation the complexes described here are included in supporting information.

2.2. Part B: Nickel and Zinc Cluster Complexes

The work was continued, and the focus was moved to the crystallisation of some different nickel and zinc cluster complexes. Again, four neodymium (NdFeB) block magnets (60 x 30 x 15 mm) and the samples were placed in 30cm^3 vials adjacent to the magnets. Initial observations were that by placing sample vials containing solubilised paramagnetic complexes alongside an MCT, the product crystallises in a patterned orientation preferentially along the MCT / sample vial interface. This was demonstrated neatly using heptanuclear *psuedo* metallocalix[6]arene complexes $[(MeOH)_2\subset Ni(II)_7(OH)_6(L)_6](NO_3)_2]$ [37] (CCDC = 758960) and $[(MeOH)_2\subset Zn(II)_7(OH)_6(L)_6](NO_3)_{2,,}$ CCDC = 758961, (where LH = 2-iminomethyl-6-methoxyphenol). [37] More specifically, the green solution of the paramagnetic Ni(II) analogue crystallised along regions of higher magnetic field as highlighted using magnetic paper (50mm x 50mm) and illustrated in Figure 8. To show that this is a paramagnetic effect, magnetic crystallisation studies on the analogous diamagnetic Zn(II) complex ($[(MeOH)_2\subset Zn(II)_7(OH)_6(L)_6](NO_3)_{2;}$ CCDC = 758961) [53] were carried out and were found to give no preferential crystal growth distribution. These observations can be more clearly observed via the video clip (see supporting information).

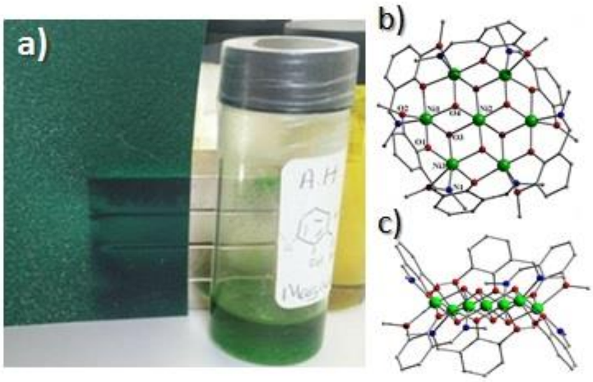

Figure 8. (a) A magnetic crystallisation tower (MCT) alongside a sample of $[(MeOH)_2\subset Ni(II)_7(OH)_6(L)_6](NO_3)_2$ (**6**) (L = 2-methoxy-6-[(E)-(methylimino)methyl]phenol; b and c), whose green hexagonal crystals are forming in alignment with the high magnetic field regions of the MCT. These regions are highlighted by the dark domains demonstrated using magnetic paper. Colour code: Ni (green), O (red), N (blue) and C (grey). Hydrogen atoms have been omitted for clarity.

For the third and final example we present the directed crystallisation of the previously reported 1-D coordination polymer $[Dy(III)(OAc)_3(MeOH)]_n$. [54,55] This was carried out by dissolving the initially prepared dimeric complex $[Dy(III)_2(OAc)_6(H_2O)_4].4H_2O$ in methanol to give a 17.46 mM solution of the resultant polymer. This methanolic solution was placed next to a MCT and over the space of 24 hours a white polycrystalline sample of $[Dy(III)(OAc)_3(MeOH)]_n$ crystallised preferentially at the sample vial – MCT interface as highlighted in Figure 9a (see accompanying video clip in ESI). An identical solution was crystallised away from the MCT, giving a uniform layer of the polymer at the bottom of the sample vial. As shown in Figures 9b and 9c, single-crystal X-ray diffraction data on this complex (CCDC = 2424601) confirmed polymer formation (CCDC = 727044; for a comparison of the unit cells see Table S8).

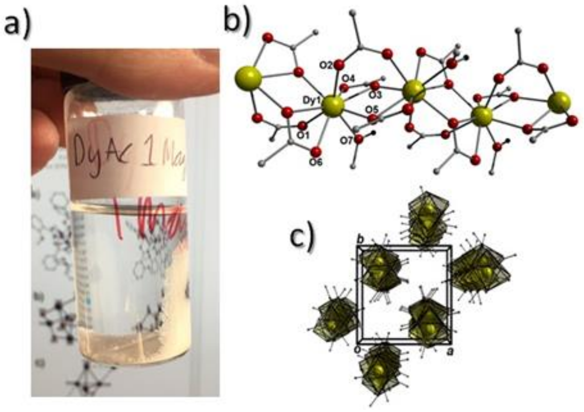

Figure 9. Photograph of the localised crystallisation of the coordination polymer [Dy(III)(OAc)$_3$(MeOH)]$_n$ [54] alongside a crystal structure representation (b) and its corresponding packing arrangements (c). Colour code: Dy (yellow), O (red), C (grey) and H (black). Most hydrogen atoms have been omitted for clarity.

3. Concluding Comments

The mechanism of the crystallisation process is of general interest. Clearly the diffusion and migration processes are of interest in addition to crystal nucleation and growth. In some test reactions it was possible to observe bulk diffusion and solution perturbations, caused directly by external magnets, however these tended to be using very strong magnets, rather than the ones described here. The nucleation process is of special interest as the initial crystallisations clearly must be directly affected by the magnetic fields – the locations of the highest concentration of metals ions in solution are likely to give rise to preferential nucleation. Thereafter the actual crystal growth also may be affected by the external field. At this point there are no general rules except that the phenomenon of crystal patterning seems to be a general one.

These findings are, to the best of our knowledge, only the second report concerning the crystallisation of paramagnetic complexes using commercially available Nd magnets and the first to construct purpose built MCTs (and other elaborate set-ups) to aid the crystallisation process. We are currently working on directing metal surface attachment of pertinent magnetic materials through the careful placement of a metal plate within the required paramagnetic solution and parallel with our MCT structure. We aim to control this surface coverage by using suitable ligands to construct target magnetic complexes. For instance, ligands with thiol or thioacetate groups at their periphery will be directed in a controlled manner via favoured Ag-S bond formation, effectively anchoring the metal complex to the gold plate. We envisage application in the surface attachment of (for instance) magnetic coolant materials as required for their effective operation. We will also crystallise known magnetically interesting materials (e.g. chiral magnetic complexes) in the presence of our MCTs to probe any resultant structural changes as even minute modifications can cause significant changes in magnetic behaviour. Clearly this work can lead to interesting scholastic activities with pupils and students using these techniques for classroom activities provided the requisite safety precautions are taken in handling magnets. It is envisaged that many metal complexes will behave in the manor described here. We also would like to use electromagnets and rotating field magnets in future experiments as well as experiments carried out directly in MRI instruments, given the implications of this work in biology, in particular brain chemistry.

4. Materials and Methods

The Materials and Methods are described in supplementary information section which includes figures showing the experimental layouts and visuals of the magnets used in the experiments.

Supplementary Materials: The following supporting information can be downloaded at: www.mdpi.com/xxx/s1, Crystallographic data with tables and a total of 27 figures, S1-S27 are available in the supporting information file.

Author Contributions: IRB: manuscript, writing editing and proofing, experimental work, project conception. RMW: experimental work. AH: experimental work. PNH: crystallography, writing and proofing. SJC: crystallography overseer. LFJ: manuscript, writing editing and proofing, experimental work, project conception.

Funding: We thank EPSRC for funding the National Crystallography Service (Southampton)
No external funding was received for the synthetic work.
Data Availability Statement: Please see S.I. section for general data availability.

Acknowledgments: We would like to thank Prof. Patrick Murphy, now Emeritus, of Bangor University for provision of time and Dr Zahraa S. Al-Taie of Al-Nahrain University, for additional help with photographing experimental set ups.

Conflicts of Interest: Declare conflicts of interest or state "The authors declare no conflict of interest."

References

1. Dechambenoit, P.; Long, J.R. Microporous magnets, *Chem. Soc. Rev.*, **2011**, *40*, 3249–3265. DOI https://doi.org/10.1039/C0CS00167H
2. Garcés-Pineda, F.A.; Blasco-Ahicart, M., Castro, N.; López, D.N.; Galán-Mascarós. J.R. Direct magnetic enhancement of electrocatalytic water oxidation in alkaline media, *Nat. Energy*, **2019**, *4*, 519–525. https://doi.org/10.1038/s41560-019-0404-4
3. Steiner, U.E.; Ulrich, T. Magnetic field effects in chemical kinetics and related phenomena, *Chem. Rev.*, **1989**, *89*, 51-147. https://doi.org/10.1021/cr00091a003
4. Yan, E.-K.; Zhang, C.-Y.; He, J.; Yin, D.-C. An Overview of Hardware for Protein Crystallization in a Magnetic Field, *Int. J. Mol. Sci.* **2016**, *17*, 1906. doi: 10.3390/ijms17111906.
5. Hu, L.; Wang, Z., Wang, H.; Qu, Z.; Chen, Q. Tuning the structure and properties of a multiferroic metal-organic-framework via growing under high magnetic fields, *RSC Adv.* **2018**, *8*, 13675-13678. doi: 10.1039/c8ra00799c.
6. Meihaus, K.R.; Corbey, J.F.; Fang, M.; Ziller, J.W.; Long, J.R.; Evans, W.R. Separating rare earth complexes using a commercial bar magnet, *Inorg. Chem.*, **2014**, *53*, 3099-3107. DOI:10.1021/ic4030102
7. Potticary, J.; Hall, C.L.; Guo, R.; Price, S.L.; Hall. S.R. On the Application of Strong Magnetic Fields during Organic Crystal Growth, *Crystal Growth & Design*, **2021**, *21*, 6254-6265. https://doi.org/10.1021/acs.cgd.1c00723
8. Wakayama, N.I. Effects of a Strong Magnetic Field on Protein Crystal Growth, *Cryst. Growth and Design*, **2003**, *3*, 17-24. https://doi.org/10.1021/cg025565g
9. Coronado, E. Molecular magnetism: from chemical design to spin control in molecules, materials and devices. *Nat Rev Mater*, **2020**, *5*, 87–104. https://doi.org/10.1038/s41578-019-0146-8
10. Chen, Y.-C.; Tong, M.-L. Single-molecule magnets beyond a single lanthanide ion: the art of coupling, *Chem. Sci.*, **2022**, *13*, 8716-8726. https://doi.org/10.1039/D2SC01532C
11. Woodruff, D.N.; Winpenny, R.E.P.; Layfield, R.A. Lanthanide single-molecule magnets, *Chem. Rev.*, **2013**, *113*, 5110−5148. doi.org/10.1021/cr400018q
12. V. Kozhevnikov. Meissner Effect: History of Development and Novel Aspects, *J. Supercond. Nov. Magn.* **2021**, *34*, 1979–2009. https://doi.org/10.1007/s10948-021-05925-8
13. Essén, H.; Fiolhais, M.C.N. Meissner effect, diamagnetism, and classical physics—a review, *Am. J. Phys.*, **2012**, *80*, 164–169. https://doi.org/10.1119/1.3662027
14. Wilcox, J.A.; Grant, M.J.; Malone, L.; Putzke, C.; Kaczorowski, D.; Wolf, T.; Hardy, F.; Meingast, C.; Analytis, J.G.; Chu, J.-H.; Fisher, I.R.; Carrington, A. Observation of the non-linear Meissner effect, *Nature Commun.*, **2022**, *13*, 1201- . https://doi.org/10.1038/s41467-022-28790-y
15. Liu, X.; Pollner, B.; Paulitsch-Fuchs, A.H.; Fuchs, E.C.; Dyer, N.P.; Loiskandl, W.; Lass-Flörl, C. Investigation of the effect of sustainable magnetic treatment on the microbiological communities in drinking water, *Environmental Research*. **2022**, *213*, 113628. https://doi.org/10.1016/j.envres.2022.113638

16. Lin, L.; Jiang, W.; Xu, P. A critical review of the application of electromagnetic fields for scaling control in water systems: mechanisms, characterization, and operation *NPJ Clean Water.* **2020**, *3*, 25. https://doi.org/10.1038/s41545-020-0071-9
17. Coey, J.M.D.; Cass S. Magnetic water treatment, *J. Magnetism and Mag. Mater.*, **2000**, *209*, 71-74. https://doi.org/10.1016/S0304-8853(99)00648-4
18. Alimi, F.; Tlili, M.M.; Ben Amor, M.; Maurin, G.; Gabrielli, C. Influence of magnetic field on calcium carbonate precipitation, *Chem. Eng and Processing: Process Intensification.* **2009**, *48*, 1327-1332. https://doi.org/10.1016/j.desal.2006.02.064
19. Wakayama, N.I. Effects of a Strong Magnetic Field on Protein Crystal Growth. *Cryst. Growth and Design.* **2003**, *3*, 17-24. https://doi.org/10.1021/cg025565g
20. Nakamura, A.; Ohtsuka, J.; Kashiwagi, T.; Numoto, Hirota, N.; Ode, T.; Okada, H.; Nagata, K.; Kiyohara, M.; Suzuki, E.; Kita, A.; Wada, H.; Tanokura, M. In-situ and real-time growth observation of high-quality protein crystals under quasi-microgravity on earth, *Sci. Reports.*, **2016**, 6, 22127. https://doi.org/10.1038/srep22127
21. Yin. D.-C. Prog. Protein crystallization in a magnetic field, *Cryst. Growth and Charact. Mat.*, **2015**, *61*, 1-26. https://doi.org/10.1016/j.pcrysgrow.2015.03.001
22. Moreno, A.; Quiroz-Garcia, B.; Yokaichiya, F.; Stojanoff, V.; Rudolph, P. Protein crystal growth in gels and stationary magnetic fields. *Cryst. Res. Technol.*, **2007**, *42*, 231-236. 10.1002/crat.200610805.
23. Maki S.; Hagiwara, M. Contactless crystallization method of protein by a magnetic force booster, *Sci. Reports.* **2022**, *12*, 17287. https://doi.org/10.1038/s41598-022-21727-x
24. Atkinson, M.B.J.; Bwambok, D.K.; Chen, J.; Chopade, P.D.; Thuo, M.M.; Mace, C.R.; Mirica, K.A.; Kumar, A.A.; Myerson, A.S.; Whitesides, G.M. Using Magnetic Levitation to Separate Mixtures of Crystal Polymorphs, *Angew. Chem. Int. Ed.* **2013**, *52*, 10208 –10211. DOI: 10.1002/anie.201305549
25. Abrahamsson, C.K; Nagarkar, A.; Fink, M.J.; Preston, D.J.; Ge, S.; Bozenko Jr, J.S.; Whitesides, G.M. Analysis of Powders Containing Illicit Drugs Using Magnetic Levitation, *Angew. Chem., Int. Ed. Engl.*, **2020**, *132*, 884-891. https://doi.org/10.1002/anie.201910177
26. L. Hu, Z. Wang, H. Wang H, Z. Qu and Q. Chen. Tuning the structure and properties of a multiferroic metal–organic-framework via growing under high magnetic fields. *RSC Adv*. **2018**, *8*, 13675-13678. DOI: 10.1039/C8RA00799C (Paper) *RSC Adv.*, 2018, **8**, 13675-13678..
27. Hong, D.L.; Luo, Y.-H.; He, Z.-T.; He, C.; Zheng, Z.-Y.; Su, S.; Wang, C.; Wang, J.-Y.; Chen, C; Sun, B.-W. Molecular Disorder Induced by the Application of an External Magnetic Field during Crystal Growth, *J. Phys. Chem.*, **2019**, *123*, 15230-15235. DOI: 10.1021/acs.jpcc.9b05010
28. Meihaus, K.R.; Corbey, J.F.; Fang, M.; Ziller, J.W.; Long, J.R.; Evans, W.J. Influence of an Inner-Sphere K+ Ion on the Magnetic Behavior of N23– Radical-Bridged Dilanthanide Complexes Isolated Using an External Magnetic Field, *Inorg. Chem.*, **2014**, *53*, 3099-3107. https://doi.org/10.1021/ic4030102
29. Higgins, R.F.; Cheisson, T.; Cole, B.E.; Manor, B.C.; Carroll, P.J.; Schelter, E.J. Magnetic Field Directed Rare-Earth Separations *Angew. Chem. Int. Ed.*, **2019**, *58*, 2-8. https://doi.org/10.1002/anie.201911606
30. Banerjee-Ghosh, K.; Dor, O.B.; Tassinari, F.; Capua, E.; Yochelis, S.; Capua, A.; Yang, S.-H.; Parkin, S.S.P.; Sarkar, S.; Kronik, L. Baczewski, L.T.; Naaman, R.; Paltiel, Y. Separation of enantiomers by their enantiospecific interaction with achiral magnetic substrates, *Science*, **2018**, *360*, 1331-1334. DOI: 10.1126/science.aar4265
31. Garcés-Pineda, F.A.; Blasco-Ahicart, M.; Nieto-Castro, D.; López, N.; Galán-Mascarós, J.R. Direct magnetic enhancement of electrocatalytic water oxidation in alkaline media, *Nature Energy*, **2019**, *4*, 519-525. https://doi.org/10.1038/s41560-019-0404-4
32. Clevenger, A.L.; Stolley, R.M.; Aderibigbe, J.; Louie, J. Trends in the Usage of Bidentate Phosphines as Ligands in Nickel Catalysis. *Chem. Revs.* **2020**, 120, 6124-6196. DOI: 10.1021/acs.chemrev.9b00682
33. Colacot, T.J. Ferrocenyl Phosphine Complexes of the Platinum Metals in Non-Chiral Catalysis. Their Applications in Carbon—Carbon and Carbon—Heteroatom Coupling Reactions. *Platinum Metals Rev.*, **2001**, 45, 22-30. https://doi.org/10.1002/chin.200213248
34. Young, D.J.; Chienb, S.W.; Hor, T.S.A. 1,1'-Bis(diphenylphosphino)ferrocene in functional molecular materials, *Dalton Trans*., **2012**, *41*, 12655-12665. https://doi.org/10.1039/C2DT31271A

doi:10.20944/preprints202502.2279.v1

35. Nataro, C.; Campbell, A.N.; Ferguson, M.A.; Incarvito, C.D.; Rheingold, A.L. Group 10 metal compounds of 1,1′-bis(diphenylphosphino)ferrocene (dppf) and 1,1′-bis(diphenylphosphino)ruthenocene: a structural and electrochemical investigation. X-ray structures of [MCl_2(dppr)] (M=Ni, Pd), *J. Organometal. Chem.*, **2003**, *673*, 47-55. https://doi.org/10.1016/S0022-328X(03)00155-4
36. Clevenger, A.L.; Stolley, R.M.; Aderibigbe, J.; Louie, J. Trends in the usage of bidentate phosphines as ligands in nickel catalysis, *Chem. Revs.*, **2020**, *120*, 6124-6196.
37. Meally, S.T.; McDonald, C.; Karotsis, G.; Papaefstathiou, G.S.; Brechin, E.K.; Dunne, P.W.; McArdle, P.; Power, N.P.; Jones L.F. A family of double-bowl pseudo metallocalix[6]arene discs, *Dalton Trans*, **2010**, 39, 4808-4816. https://doi.org/10.1039/b926704b
38. Meally, S.T.; Karotsis, G.; Brechin, E.K.; Papaefstathiou, G.S.; Dunne, P.W.; McArdle, P., Jones, L.F. Planar [Ni_7] discs as double-bowl, pseudo metallacalix[6]arene host cavities, *Cryst. Eng. Comm.*, **2010**, *12*, 59-63. DOI:10.1039/B914538A
39. Hazari, N., Melvin, P.; Beromi, M. Well-defined nickel and palladium precatalysts for cross-coupling, *Nat. Rev. Chem.*, **2017**, ***1***, 0025. https://doi.org/10.1038/s41570-017-0025
40. Casellato, U.; Ajó, D.; Valle, G.; Corain, B.; Longato, B.; Graziani, R. Heteropolymetallic complexes of 1,1′-bis(diphenylphosphino) ferrocene (dppf). II. Crystal structure of dppf and $NiCl_2$(dppf), *J. Cryst. Spect. Res.*, **1988**, *18*, 583–590. https://doi.org/10.1007/BF01161151
41. This complex [C_6H_4-CH_2PtBu_2¬-2-C_6H_4-$CH_2P(H)tBu_2)_2NiCl_3$, is prepared reaction of the ligand [1,2-C_6H_4-$(CH_2PtBu_2)_2$] with [Ni(DME) $NiCl_2$] in dichloromethane. Further information is included in supplementary materials.
42. Hashimoto, T.; Ishimaru, T.; Shiota, K.; Yamaguchi, Y. Bottleable $NiCl_2$(dppe) as a catalyst for the Markovnikov-selective hydroboration of styrenes with bis(pinacolato)diboron. *Chem. Commun.*, **2020**, 56, 11701-11704. DOI https://doi.org/10.1039/D0CC05246A
43. Busby, R.; Hursthouse, M.B.; Jarrett, P.S.; Lehmann, C.W.; Malik, K.M.A.; Phillips, C. Dimorphs of [1,2-bis(diphenylphosphino)ethane]dichloronickel(II), *J. Chem. Soc., Dalton Trans.*, **1993**, 3767-3770 DOI https://doi.org/10.1039/DT9930003767
44. Ramaswamy, H.N.; Jonassen, H.B.; Aguiar, A.M., Nickel (II) and cobalt (II) complexes of cis - 1,2, bis (diphenylphosphino) ethylene, *Inorg. Chim. Acta,* **1967**,*1*, 141-144. https://doi.org/10.1016/S0020-1693(00)93156-6.
45. Van Hecke, G.R; Horrocks, W.D. Ditertiary Phosphine Complexes of Nickel. Spectral, Magnetic, and Proton Resonance Studies. A Planar-Tetrahedral Equilibrium, *Inorg. Chem.* 1966, **5**, 1968–1974. DOI:10.1021/IC50045A029
46. For an extensive review on Nickel phosphines in catalysis see: Clevenger, A.L.; Stolley, R.M.; Aderibigbe, J.; Louie, J., Trends in the Usage of Bidentate Phosphines as Ligands in Nickel Catalysis. *Chem. Rev.* 2020, **120**, 6124-6196. https://doi.org/10.1021/acs.chemrev.9b00682
47. Davis, R., Fergusson, J.E. Coordination chemistry of 1,1,1-tris-(bisphenylphosphinomethyl) ethane. II. Four and five coordinate complexes of cobalt(II) and nickel(II), *Inorg. Chim. Acta.*, **1970**, *4*, 23-28. https://doi.org/10.1016/S0020-1693(00)93233-X
48. de Assis, E.F.; Filgueiras, C.A.L.,1,1,1- Tris(diphenylphosphinemethyl)ethane complexes of nickel and platinum with tin, *Transition Met. Chem.*, **1994**, *19*, 484-486. https://doi.org/10.1007/BF00136355
49. Hu, C.; Chew, R.J.; Tang, H.M.; Madrahimov, S.; Bengali, A.A.; Fan, W.Y. Triphos nickel(II) halide pincer complexes as robust proton reduction electrocatalysts. *Mol. Catalysis*, 2020, 490, 110950-https://doi.org/10.1016/j.mcat.2020.110950
50. Dapporto, P.; Midollini, S.; Orlandini, A.; Sacconi, L. Complexes of cobalt, nickel, and copper with the tripod ligand 1,1,1-tris(diphenylphosphinomethyl)ethane (p3). Crystal structures of the [Co(p3)(BH_4)] and [Ni(p3)(SO_2)] complexes, *Inorg. Chem.*, **1976**, *15*, 2768-2774. DOI: 10.1021/ic50165a040
51. Kandiah, M.; McGrady, G.S. ; Decken, A.; Sirsch, P. [(Triphos)Ni(η2-BH4)]: An Unusual Nickel(I) Borohydride Complex, *Inorg. Chem.*, **2005**, *44*, 8650-8652. DOI: 10.1021/ic051541y
52. Kato, H.; Yorita, K.; Kato, Y.; Structural lnterconversions of Dichlorobis(triphenylphosphine)- nickel(II) in Various Solvents. *Bull. Chem. Soc. Jpn.*, **1979**, 52, 2465-2473. DOI:10.1246/BCSJ.52.2465

53. Meally, S.T.; McDonald, C.; Kealy, P.; Taylor, S.M.; Brechin, E.K.; Jones, L.F. Investigating the solid state hosting abilities of homo- and hetero-valent [Co-7] metallocalix[6]arenes, *Dalton Trans.*, **2012**, *41*, 5610-5616. https://doi.org/10.1039/c2dt12229
54. Baggio, R.; Munoz, J.C.; Perec, M. Bis(μ-acetato-κ^3*O*,*O*′:*O*′)bis[bis(acetato-κ^2*O*,*O*′)diaquadysprosium(III)] tetrahydrate, *Acta. Cryst. C.* **2002**, C58, m498-m500. https://doi.org/10.1107/S010827010201510X
55. Zheng, Y.-Z.; Lan, Y.; Wernsdorfer, W.; Anson, C.E.; Powell, A.K. Polymerisation of the Dysprosium Acetate Dimer Switches on Single-Chain Magnetism. *Chem. Eur. J.* **2009**, *15*, 12566-12570. https://doi.org/10.1002/chem.200902064